Revisiting Abnormalities in Brain Network Architecture Underlying Autism Using Topology-Inspired Statistical Inference

Sourabh Palande, Vipin Jose, Brandon Zielinski, Jeffrey Anderson, P. Thomas Fletcher, and Bei Wang

University of Utah

Abstract

A large body of evidence relates autism with abnormal structural and functional brain connectivity. Structural covariance MRI (scMRI) is a technique that maps brain regions with covarying gray matter density across subjects. It provides a way to probe the anatomical structure underlying the intrinsic connectivity networks (ICNs) through analysis of the gray matter signal covariance. In this paper, we apply topological data analysis in conjunction with scMRI to explore network-specific differences in the gray matter structure in subjects with autism versus age-, gender- and IQ-matched controls. Specifically, we investigate topological differences in gray matter structure captured by structural covariance networks (SCNs) derived from three ICNs strongly implicated in autism, namely, the salience network (SN), the default mode network (DMN) and the executive control network (ECN). By combining topological data analysis with statistical inference, our results provide evidence of statistically significant network-specific structural abnormalities in autism, in SCNs derived from SN.

1 Introduction

Autism is a complex developmental disorder characterized by impairment in social interactions, difficulty in verbal and nonverbal communications and repetitive behaviors. Although the exact mechanism of its development remains unclear, there is strong evidence relating autism to abnormal white matter and functional connectivity between brain regions. Structural abnormalities can be identified using voxel-based morphometry by comparing gray matter, white matter volumes, cortical thicknesses and their growth trajectories [11] across diagnostic groups. Although the gross brain differences have been well-documented [4], investigations into specific regional abnormalities in brain structure have reported divergent results [14].

These inconsistent findings, however, may reflect discrete abnormalities in the brain network. Research has revealed a finite set of canonical domain-specific *resting state* or *intrinsic connectivity networks* (ICNs) that organize the brain function [7]. Many of the regions with reported abnormalities in autism lie within these ICNs. Network-specific differences could account for seemingly contradictory findings from previous studies.

Structural covariance MRI (scMRI) maps regions of gray matter that have a statistically significant correlation with a specific seed region of interest (ROI) across subjects. This suggests shared developmental or genetic influences between the gray matter region and the seed ROI. Seeley et al. [12] have used scMRI to demonstrate that specific brain disorders affect distinct ICNs and the corresponding gray matter regions. Using a similar technique, Zielinski et al. [16] have shown that

there are network-specific structural differences between autism and control groups which are consistent with clinical aspects of the disease and that reported functional abnormalities in autism have a structural bias. Several recent studies have applied the scMRI technique to find network-specific structural abnormalities in other diseases such as Alzheimer's [9] and Huntington's [8].

However, scMRI can only reveal shared influences between gray matter region and a specific seed ROI. We can model all pairwise correlations across subjects, among the gray matter regions identified by the seed-based covariance map, as a network. Such networks represent structural relationships between regions which are not captured by scMRI. Comparing these networks across diagnostic groups may provide information that is not given by direct comparisons between individual regions.

Comparing networks is not an easy problem, specially when the networks are weighted. Several graph-theoretic measures have been proposed previously to compare networks [2]. However, a major drawback of these measures is their reliance on a fixed network topology. That is, these measures are typically based on a graph obtained by thresholding the connectivity matrix. The choice of threshold is crucial in such analyses. Different heuristics have been suggested to determine the threshold depending on which properties of the network are of interest. However, it is often not possible to determine a unique optimal threshold.

In this paper, we apply topological data analysis to structural covariance networks (SCNs) derived from three ICNs strongly implicated in autism; the default mode network (DMN), the salience network (SN) and the executive control network (ECN). Our method is based upon a core technique from topological data analysis known as *persistent homology* [5] where we extract topological features across all thresholds from a given network and make statistical inference by comparing these features. By combining topological data analysis with statistical inference, our results provide evidence of statistically significant structural abnormalities underlying SN in autism. Our results are consistent with the observations of Zielinski et al. [16] and may offer new insights towards interpreting fine-scale network-specific structural differences.

2 Technical Background

2.1 Structural Covariance Network

We use scMRI to identify a set of brain regions, underlying a specific *intrinsic connectivity network* (ICN). This is done by first determining a seed ROI which typically anchors a specific ICN and then finding regions that have covarying gray matter densities across subjects, with that seed ROI. Specifically, given a seed ROI, separate condition-by-covariate analysis is performed for each gray matter region. The mean seed gray matter density is the covariate of interest and disease status is the grouping variable. Total brain volume (TBV) is included as a covariate-of-no-interest. This design enables us to determine the whole-brain patterns of seed-based structural covariance in each group. To identify regions with significant gray matter density covariance with the seed ROI across subjects in a diagnostic group, one-sample t-tests with family-wise error correction are performed.

The regions are identified on the basis of their structural relationship with a specific seed ROI. We model the structural relationships between pairs of regions as a network. Correlations between gray matter densities across subjects, for all pairs of regions, are modeled as a weighted, undirected graph $G(V, E, W)$. The vertices of the graph represent gray matter regions and the edge weights are given by absolute values of pairwise correlations.

In what follows, we refer to such a network as the structural covariance network (SCN). We compare SCNs derived from three intrinsic connectivity networks strongly implicated in autism, the SN, the ECN and the DMN. In the context of this paper, for simplicity (unless otherwise specified),

we describe these SCNs by the name of their corresponding ICNs, namely, SN-SCN, ECN-SCN and DMN-SCN.

2.2 Graph Filtration

We extract topological features at multiple scales from a structural covariance network G by applying topological data analysis to a nested sequence of graphs constructed from G, referred to as the graph filtration.

Let $V = \{v_i \mid i = 1, \ldots, n\}$ be the vertex set with n vertices. Let E denote the edge set and W denote the set of edge weights. The edge between vertices v_i, v_j is denoted by e_{ij} and its weight is denoted by w_{ij}. $|E|$ denotes the number of edges. For a given threshold λ, we obtain a binary graph G_λ by removing edges with weight $w_{ij} \leq \lambda$. The adjacency matrix $A_\lambda = (a_{ij}(\lambda))$ is given by:

$$a_{ij}(\lambda) = \begin{cases} 0 & w_{ij} \leq \lambda \\ 1 & o.w. \end{cases}$$

As λ increases, more and more edges are removed from the graph. We can generate a sequence of thresholds, $\lambda_0 = 0 \leq \lambda_1 \leq \lambda_2 \leq \cdots \leq \lambda_q$, where $q \leq |E|$ by setting λ_i's equal to edge weights arranged in ascending order.

Corresponding to the sequence of thresholds we get a nested sequence of binary graphs, referred to as a *graph filtration* **G**:

$$G_{\lambda_0} \supseteq G_{\lambda_1} \supseteq G_{\lambda_2} \supseteq \cdots \supseteq G_{\lambda_q}.$$

We can measure the connectivity of a graph by its 0-th Betti number, β_0, which is the number of connected components in the graph. As the threshold λ increases, $\beta_0(G_\lambda)$ of the corresponding graph also increases. The number of connected components of the graphs in filtration **G** form a monotonic sequence of integers,

$$\beta_0(G_{\lambda_0}) \leq \beta_0(G_{\lambda_1}) \leq \beta_0(G_{\lambda_2}) \leq \cdots \leq \beta_0(G_{\lambda_q}).$$

Assuming that we started with a connected graph $G = G_{\lambda_0}$, we have $\beta_0(G_{\lambda_0}) = 1$ and $\beta_0(G_{\lambda_q}) = |V| = n$ by construction. The plot of $\beta_0(G_\lambda)$ as a function of threshold λ is called the β_0 curve. Given a finite graph with n nodes, there are at most $\binom{n}{2}$ unique edge weights. If we choose the set of all the unique edge weights, sorted in ascending order, to be the thresholds, then with finitely many threshold values, we can estimate the β_0 curve for all λ. Computing the β_0 curve for a given graph could follow the standard algorithm for persistent homology [5]. In practice, a simpler algorithm relying on the notion of a minimum spanning tree can be used to capture the λ values when we are only concerned with tracking the number of components (clusters) during the filtration.

2.3 Statistical Inference

Our data consists of subjects divided into two diagnostic groups (a.k.a., samples), autism and control. We would like to test whether the two samples come from the same underlying distribution or not. More specifically, we want to test whether there are any statistically meaningful differences in the 0-dimensional topology of the SCNs derived from the two samples. We do this by examine the equivalence among the corresponding β_0 curves.

Let G and H represent the SCNs obtained from autism and control samples respectively with corresponding graph filtrations **G** and **H**. We want to test the null hypothesis,

$$H_0 : \beta_0(G_\lambda) = \beta_0(H_\lambda) \quad \text{for all } \lambda,$$

against the alternative hypothesis,

$$H_1 : \beta_0(G_\lambda) \neq \beta_0(H_\lambda) \quad \text{for some } \lambda.$$

Since we are dealing with finite graphs, a discrete version of the null hypothesis is stated as,

$$H_0 : \beta_0(G_{\lambda_i}) = \beta_0(H_{\lambda_i}) \quad \text{for all } \lambda_i,\ i = 1, 2, \ldots, q,$$

with the null hypothesis being

$$H_1 : \beta_0(G_{\lambda_i}) \neq \beta_0(H_{\lambda_i}) \quad \text{for some } \lambda_i,\ i = 1, 2, \ldots, q.$$

Following the formulation of Chung et al. [3], we can define the distance between graph filtrations **G** and **H** as:

$$D_q(\mathbf{G}, \mathbf{H}) = \sup_{0 \leq i \leq q} |\beta_0(G_{\lambda_i}) - \beta_0(H_{\lambda_i})|. \tag{1}$$

Intuitively, D_q measures the largest gap between the two β_0 curves. The p-value is the probability that D_q will take a value equal to or greater than the observed value under the null hypothesis. In order to determine this p-value, we need to sample the distribution of D_q under the null hypothesis.

Permutation test provides a simple way to estimate such a sampling distribution. Let D_q^* denote the value computed from the two original samples. To estimate the sampling distribution of D_q, in each permutation, we randomly swap subject labels between the two groups and proceed with the following:

1. Construct SCNs for autism and control groups separately;
2. Apply graph filtration to both networks and obtain their corresponding β_0 curves;
3. Compute the corresponding D_q with the above permutation.

Each permutation gives us a new value of D_q. For a reliable estimation of the distribution of D_q, large number of permutations is required. The p-value is given by the fraction of D_q values greater than or equal to D_q^*.

3 Methods

3.1 Data Preprocessing

We derive our SCNs from the ICNs previously reported by Zielinski et al. [16, 17]. Here, we review the preprocessing pipeline. 49 male subjects with autism, aged 3-22 years, are compared to 49 age-, gender- and IQ-matched typically developing control subjects. Images are acquired using a Siemens 3.0 Tesla Trio MRI scanner. Whole brain isotropic MPRAGE image volumes are acquired in the sagittal plane using an 8-channel receive-only RF head coil, employing standard techniques (TR = 2300 ms, TE median = 3 ms, matrix median = $256 \times 256 \times 160$, flip angle = 12°, voxel resolution = 1 mm^3, acquisition time = 9 min 12 sec).

Customized image analysis templates are created by normalizing, segmenting and averaging T1 images using SPM5 according to the processing pipeline proposed in [1, 15]. First, images are transformed into standard space using a 12-parameter affine-only linear transformation and segmented into three tissue classes representing gray matter, white matter and cerebrospinal fluid. Then smoothly varying intensity changes as well as artifactual intensity alterations as a result of the

normalization step are corrected for using a standard modulation algorithm within SPM5. Finally, the resulting segmented maps are smoothed using a 12-mm full-width at half-maximum Gaussian kernel.

In performing the scMRI analysis, a two-pass procedure is utilized, wherein study-specific templates are first created by segmenting our sample using a canonical pediatric template. Then tissue-specific prior probability maps are created from our sample. The tissue compartments are then re-segmented using this sample-specific template, so that the age range of our sample precisely matches that of the template(s) upon which the ultimate segmentations are based.

3.2 Structural Covariance Networks and Statistical Inference

We would like to construct SCNs that capture structural relationships, across subjects, between all pairs of gray matter regions from a predefined set of regions. We begin by constructing a *whole brain* SCN as follows: 1-mm spheres are placed at grid points of a uniform grid on the entire preprocessed image volume. After applying the gray matter mask, we obtain a set of 7266 regions. The *whole-brain* SCN (denoted Global-SCN) is constructed by computing correlations, across subjects, between all pairs of these regions.

To study network-specific structural covariance, 4-mm-radius spherical seed ROIs are selected within the right frontoinsular cortex (R FI) [12], the right dorsolateral prefrontal cortex (R DLPC) [13] and the right posterior cingulate cortex (R PCC) [6]. These regions anchor the salience network (SN), the executive control network (ECN) and the default-mode network (DMN), respectively [12, 6].

For each diagnostic group and each seed ROI, we obtain the set of regions covarying with the seed ROI, following the process described in Section 2. The structural covariance maps corresponding to the seed ROI are shown in Fig. 1(a)-(c). Further comparisons in Fig. 2 show that the maps for two diagnostic groups do not completely overlap. Some regions present in the map for the control group are absent in the map for the autism group. Conversely, some regions are present only in the map for the autism group but not in the map for the control group. Fig. 1(d) lists the number of regions present in controls but not in autism, in autism but not in controls and in both as well as in either autism or control. A network specific set of ROIs is given by the union of all regions covarying with the corresponding seed ROI, in either the autism group map or the control group map.

Thus, we have one *Global* set of ROIs and three network specific sets of regions. For each set of ROIs, we perform the permutation test as described in section 2. One million permutations are performed in case of network-specific ROIs. Only ten thousand permutations are performed for the Global-SCN due to computational constraints.

4 Results

We apply the permutation test and compare SCNs across groups of subjects with autism and typically developing control subjects. We begin by comparing the global SCNs composed of 7266 gray matter regions in the preprocessed images. For a closer analysis, we compare the SCNs generated with seed ROIs anchoring the three ICNs (SN, ECN and DMN), referred to as SN-SCN, ECN-SCN and DMN-SCN, respectively. Recall that the structural covariance maps for the autism and the control groups overlap in very few regions. We construct and compare SCNs derived from sets of regions that are present in either controls or in autism.

The β_0 curves corresponding to the global SCNs and the seed-specific SCNs are shown in Fig. 3. Table 1 lists the p-values obtained after the permutation test. By combining topological data

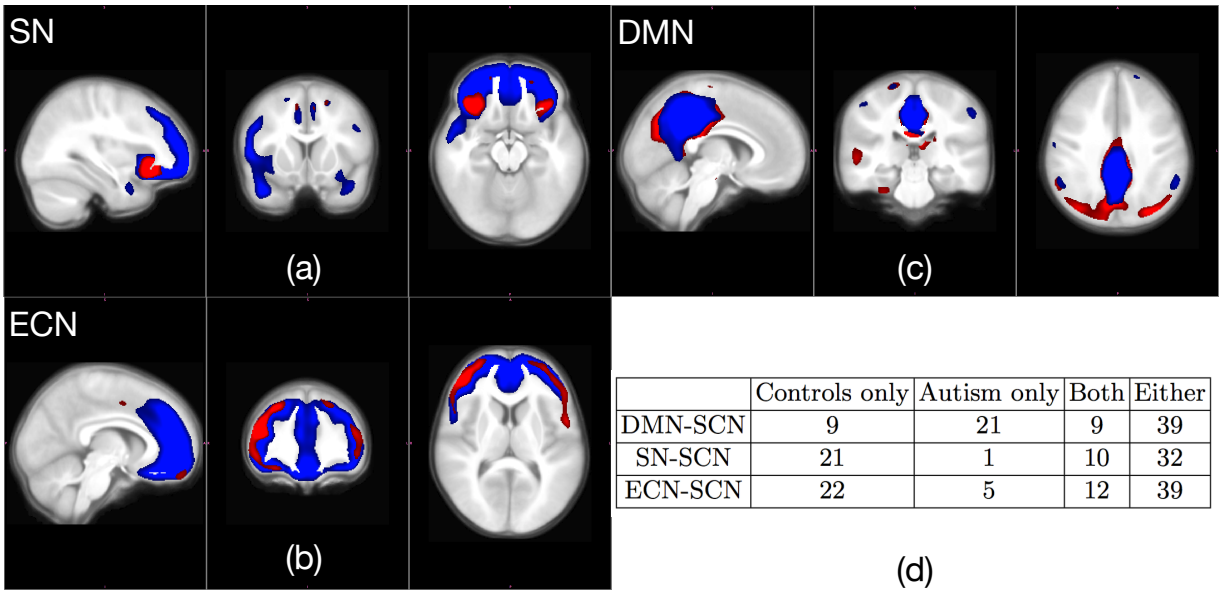

	Controls only	Autism only	Both	Either
DMN-SCN	9	21	9	39
SN-SCN	21	1	10	32
ECN-SCN	22	5	12	39

(d)

Figure 1: (a)-(c) Structural covariance maps with seed in R FI, R DLPC and R PCC, anchoring SN, ECN and DMN, respectively. Red represents the autism group map, blue represents the control group map. (d) Number of regions identified from scMRI map for a given seed region.

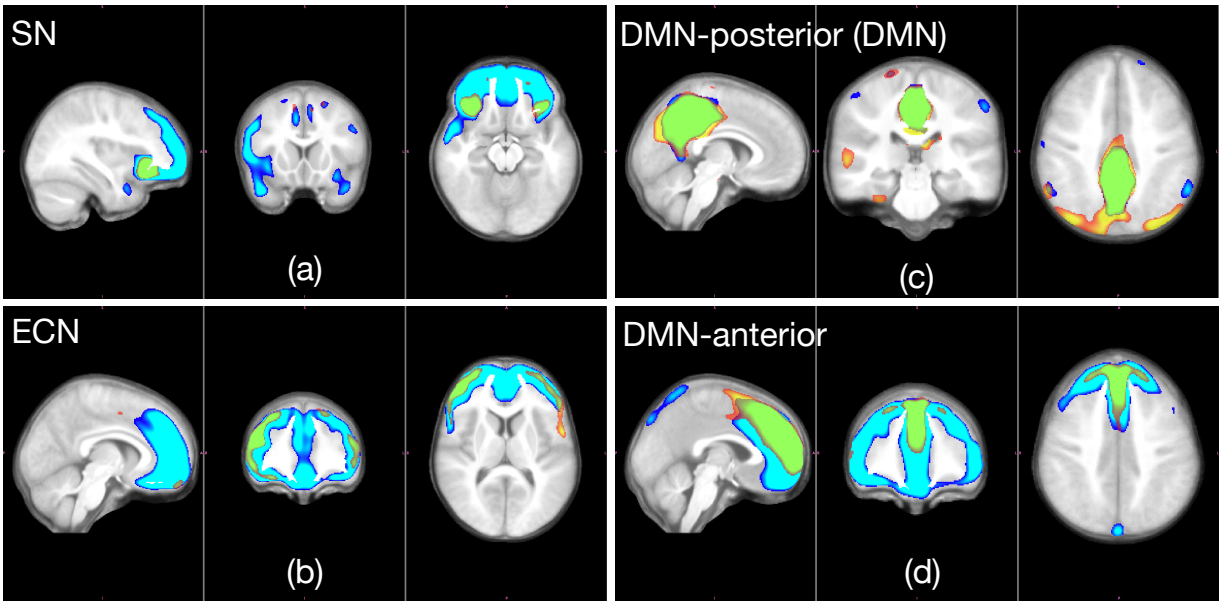

Figure 2: scMRI maps are further illustrated here with red to yellow (autism) and dark blue to light blue (control) color look up tables. The color gradation indicates increasing statistical significance. The overlapping regions among the autism and control groups are highlighted in green. Note for (c) and (d): Our data consists of subjects with an average age of about 13 years. The underlying structure of the DMN is not fully developed at this age. We include two DMN maps with different seeds to show that the posterior part (c) is not yet integrated with the anterior part (d). In our analysis, we use the posterior covariance map (c) which corresponds to the most common seed for DMN in adults (R PCC).

analysis with statistical inference, our results provide evidence of statistically significant network-specific structural abnormalities in autism SN-SCNs.

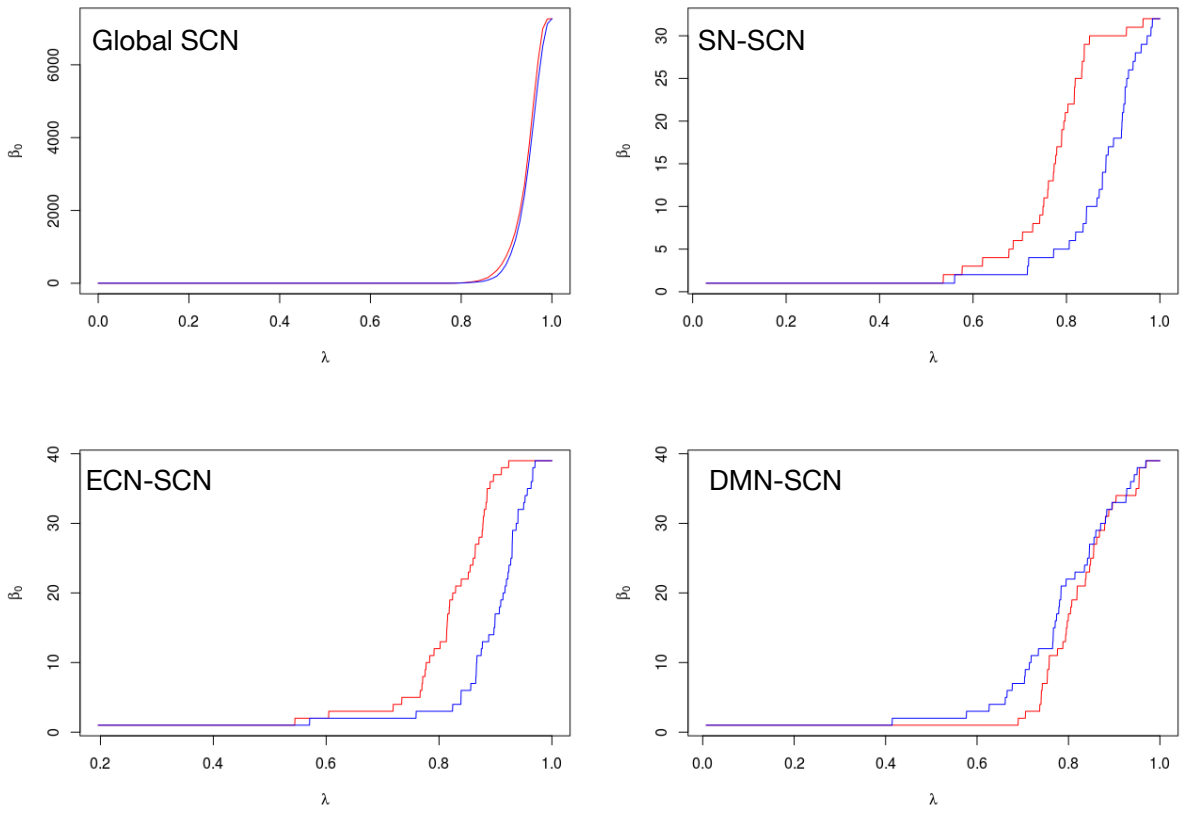

Figure 3: β_0 curves from Global SCNs as well as SN-SCNs, ECN-SCNs and DMN-SCNs, generated from regions present in either autism (red) or controls (blue) respectively.

	Global-SCN	DMN-SCN	SN-SCN	ECN-SCN
p-value	0.3985	0.3658	**0.00614**	0.1118

Table 1: p-values for permutation test on SCNs

5 Comparison and Discussion with Respect to Prior Work

In an earlier version of this work [10], we used an exact statistical inference method first proposed in [3]. It is derived from the two sample Kolmogorov-Smirnov (KS) test, based on the fact that the β_0 sequences are monotonic increasing sequences. Here we will briefly review the two sample KS test and discuss why the inference method we used in [10] was in fact, not appropriate in our setting.

5.1 Two sample KS Test

Suppose there exist two populations X and Y with cumulative distribution functions F_X and F_Y respectively. Given a random (i.i.d.) sample from X and a random sample from Y, we wish to test whether the populations are identical or not, i.e.

$$H_0 : F_X(x) = F_Y(x) \quad \forall x,$$

against the alternative

$$H_1 : F_X(x) \neq F_Y(x) \quad \text{for some } x.$$

F_X and F_Y are assumed to be continuous. For simplicity, let us also assume that both samples are of the same size n. Let the order statistic of the samples be

$$X_{(1)}, X_{(2)}, \ldots, X_{(n)} \quad \text{and} \quad Y_{(1)}, Y_{(2)}, \ldots, Y_{(n)}.$$

The empirical distribution function of the samples, denoted $S_n(x)$ and $T_n(x)$ are the proportions of samples with values smaller than or equal to x. They are step functions that increase by $1/n$ at the jump points which coincide with the order statistic of the respective samples. Formally, $S_n(x)$ is defined as

$$S_n(x) = \begin{cases} 0 & \text{if } x < X_{(1)} \\ \frac{k}{n} & \text{for } X_{(k)} \leq x \leq X_{(k+1)}, \text{ where } k = 1, 2, \ldots, n-1 \\ 1 & \text{if } x \geq X_{(n)} \end{cases}$$

For a fixed, but arbitrary value of x, $S_n(x)$ itself is a random variable with following properties:

1. $nS_n(x)$ follows a binomial distribution with parameter $\theta = F_X(x)$, that is,

$$P[S_n(x) = j/n] = \binom{n}{j} [F_X(x)]^j [1 - F_X(x)]^{n-j}$$

2. $E[S_n(x) = F_X(x)]$ and $\text{Var}[S_n(x)] = \frac{F_X(x)[1-F_X(x)]}{n}$

3. **Glivenko-Cantelli Theorem:** $S_n(x)$ converges uniformly to $F_X(x)$. That is, for every $\epsilon > 0$

$$\lim_{n\to\infty} P[\sup_{-\infty<x<\infty} |S_n(x) - F_X(x)| > \epsilon] = 0$$

4. As $n \to \infty$, standardized $S_n(x) \approx$ standard normal distribution.

The properties mentioned above ensure that $S_n(x)$ and $T_n(x)$ are reasonable estimates of $F_X(x)$ and $F_Y(x)$ respectively. Under the null hypothesis, two populations being identical implies that the two samples are drawn i.i.d. from the same distribution. Therefore, the two empirical distributions should agree. The KS two sample test statistic is given as:

$$D_{n,n} = \max_x |S_n(x) - T_n(x)|.$$

For any continuous F_X and F_Y and random samples drawn from the two populations, $D_{n,n}$ is completely distribution free. The exact and asymptotic probability distributions for $D_{n,n}$ are derived using this fact and the properties of empirical distribution functions mentioned earlier.

5.2 Issues with previous inference method

The underlying assumption of the exact inference method used in [10] was that the two β_0 sequences, after normalization, could be used as empirical distribution functions in the two sample KS test, the KS statistic being D_q as defined in 1.

The empirical distribution functions are derived from random samples. They are step functions with jump points coinciding with the order statistics of the samples. The normalized β_0 curves are step functions with exactly n jumps, but for them to be used as empirical distribution functions, the order statistics would have to be the n threshold values at which the jumps in β_0 curves occur. These are the values at which the number of connected components changes. A closer examination of the setup reveals the following:

1. The order statistics in this case are independent of the number of subjects. The number of jumps in the β_0 curves is determined by the number of nodes in the SCNs. The number of samples is determined by the number of gray matter ROIs instead of the number of autism and control subjects. We cannot use such a test to infer anything about the autism and control populations.

2. The results on exact as well as asymptotic null distribution of the KS statistic follow from the fact that it is distribution free. Given a weighted undirected graph G, the threshold values at which jumps in the β_0 curve occur are uniquely determined and not i.i.d. as required by the KS test. As a consequence, we can no longer claim that the D_q is distribution free to construct a KS test with D_q as a test statistic.

These two issues make it clear that the inference method employed in [10] was not appropriate for the hypotheses we would like to test.

6 Conclusion

Using direct comparisons of structural covariance maps, Zielinski et al. have shown the structural differences in gray matter regions underlying *intrinsic connectivity networks* (ICNs) such as SN [16], DMN [16] and ECN (Brandon Zielinski, personal communication, May 2017), between the autism and the control groups.

A key insight from their work is that structure enables function and functional collaboration enables structure. Our work helps to summarize these multidimensional, structure-function relationships by conceptualizing them as higher-order topological relationships.

The techniques in [16] compare covariance maps directly. The regions in these maps are assigned significance measures based on their covariance with respect to the specified seed region. The SCNs, on the other hand, encode all pairwise associations among regions, where the extent of an association is measured by the correlations across subjects. Our experiments provide evidence of statistically significant differences in the 0-dimensional topological features of SCNs derived from SN (SN-SCNs). This result is consistent with the findings of Zielinski et al. [16].

However, it should be noted that the SCNs are abstract networks and do not represent physical connectivity between the regions. This limits the interpretability of our results to some extent and deeper analysis is needed in order to quantify and better interpret the differences suggested by the statistical inference.

Our method, fails to capture any significant differences in the topology of SCNs derived from DMN or ECN (DMN-SCNs, ECN-SCNs). It is possible that considering only pairwise interactions among gray matter regions (that is, 0-order topological features encoded by the β_0 curves, corresponding to the number of connected components) may not be sufficient to capture the complex topological differences within these SCNs. Analyzing three-way or four-way interactions, capturing higher-order topological features such as tunnels and voids and focusing on specific sites directly involved in merging components in the graph filtration may provide further insights into these SCNs.

Acknowledgements. This work was supported by NIH grant R01EB022876 and NSF grant IIS-1513616.

References

[1] M. Altaye, S. K. Holland, M. Wilke, and C. Gaser. Infant brain probability templates for {MRI} segmentation and normalization. *NeuroImage*, 43(4):721 – 730, 2008.

[2] E. Bullmore and O. Sporns. Complex brain networks: graph theoretical analysis of structural and functional systems. *Nature Reviews Neuroscience*, 10(3):186–198, 2009.

[3] M. K. Chung, V. Villalta-Gil, H. Lee, P. J. Rathouz, B. B. Lahey, and D. H. Zald. Exact topological inference for paired brain networks via persistent homology. *bioRxiv:140533*, 2017.

[4] E. Courchesne, K. Pierce, C. M. Schumann, E. Redcay, J. A. Buckwalter, D. P. Kennedy, and J. Morgan. Mapping early brain development in autism. *Neuron*, 56(2):399 – 413, 2007.

[5] H. Edelsbrunner, D. Letscher, and A. J. Zomorodian. Topological persistence and simplification. *Discrete and Computational Geometry*, 28:511–533, 2002.

[6] D. A. Fair, A. L. Cohen, N. U. F. Dosenbach, J. A. Church, F. M. Miezin, D. M. Barch, M. E. Raichle, S. E. Petersen, and B. L. Schlaggar. The maturing architecture of the brain's default network. *Proceedings of the National Academy of Sciences*, 105(10):4028–4032, 2008.

[7] M. D. Fox, A. Z. Snyder, J. L. Vincent, M. Corbetta, D. C. Van Essen, and M. E. Raichle. The human brain is intrinsically organized into dynamic, anticorrelated functional networks. *Proceedings of the National Academy of Sciences of the United States of America*, 102(27):9673–9678, 2005.

[8] L. Minkova, S. B. Eickhoff, A. Abdulkadir, C. P. Kaller, J. Peter, E. Scheller, J. Lahr, R. A. Roos, A. Durr, B. R. Leavitt, S. J. Tabrizi, S. Klöppel, and T.-H. Investigators. Large-scale brain network abnormalities in huntington's disease revealed by structural covariance. *Human Brain Mapping*, 37(1):67–80, 2016.

[9] M. Montembeault, I. Rouleau, J.-S. Provost, and S. M. Brambati. Altered gray matter structural covariance networks in early stages of alzheimer's disease. *Cerebral Cortex*, 26(6):2650, 2016.

[10] S. Palande, V. Jose, B. Zielinski, J. Anderson, P. T. Fletcher, and B. Wang. *Revisiting Abnormalities in Brain Network Architecture Underlying Autism Using Topology-Inspired Statistical Inference*, pages 98–107. Springer International Publishing, 2017.

[11] C. M. Schumann, C. S. Bloss, C. C. Barnes, G. M. Wideman, R. A. Carper, N. Akshoomoff, K. Pierce, D. Hagler, N. Schork, C. Lord, and E. Courchesne. Longitudinal magnetic resonance imaging study of cortical development through early childhood in autism. *Journal of Neuroscience*, 30(12):4419–4427, 2010.

[12] W. W. Seeley, R. K. Crawford, J. Zhou, B. L. Miller, and M. D. Greicius. Neurodegenerative diseases target large-scale human brain networks. *Neuron*, 62:42–52, 04 2009.

[13] W. W. Seeley, V. Menon, A. F. Schatzberg, J. Keller, G. H. Glover, H. Kenna, A. L. Reiss, and M. D. Greicius. Dissociable intrinsic connectivity networks for salience processing and executive control. *Journal of Neuroscience*, 27(9):2349–2356, 2007.

[14] K. A. Stigler, B. C. McDonald, A. Anand, A. J. Saykin, and C. J. McDougle. Structural and functional magnetic resonance imaging of autism spectrum disorders. *Brain Research*, 1380:146–161, 03 2011.

[15] M. Wilke, S. K. Holland, M. Altaye, and C. Gaser. Template-o-matic: A toolbox for creating customized pediatric templates. *NeuroImage*, 41(3):903 – 913, 2008.

[16] B. A. Zielinski, J. S. Anderson, A. L. Froehlich, M. B. D. Prigge, J. A. Nielsen, J. R. Cooperrider, A. N. Cariello, P. T. Fletcher, A. L. Alexander, N. Lange, E. D. Bigler, and J. E. Lainhart. scmri reveals large-scale brain network abnormalities in autism. *PLOS ONE*, 7(11):1–14, 11 2012.

[17] B. A. Zielinski, E. D. Gennatas, J. Zhou, and W. W. Seeley. Network-level structural covariance in the developing brain. *Proceedings of the National Academy of Sciences*, 107(42):18191–18196, 2010.